RESEARCH ARTICLE

Pedestrian Trajectory Reconstruction for Indoor Movement Based on Foot-Mounted IMU

Yeqing Wang[1] **and Binbin Wang**[1,*]

[1] National Engineering Laboratory for Agri-product Quality Traceability, BTBU, Beijing, China

Abstract

A pedestrian navigation system (PNS) that only relies on the foot-mounted IMU is useful for various applications, especially under some severe conditions, such as tracking of firefighters and miners. Due to the complexity of the indoor environment, signal occlusion problems could lead to the failure of certain positioning methods. In complex environments such as fire rescue and emergency rescue, the barometric altimeter fails because of the influence of air pressure and temperature. This paper used an improved zero velocity detection algorithm to improve the accuracy of gait detection. Then, combine the Kalman filter with the zero velocity update algorithm to recognize gait accurately and take corresponding actions. Finally, the trajectory involving both horizontal and vertical movement was obtained. The proposed method avoids the redundancy associated with multi-sensor data fusion and can be used in complex unknown environments.

Keywords: pedestrian navigation, zero-velocity detection, Kalman filter, foot-mounted IMU.

Academic Editor:
Weimin Zhang

Submitted: 03 February 2024
Accepted: 20 May 2024
Published: 26 May 2024

Vol. 1, **No.** 1, 2024.
10.62762/TIS.2024.136995

***Corresponding author:**
✉ Binbin Wang
wangbinbin@st.btbu.edu.cn

1 Introduction

Pedestrian navigation refers to the user completing real-time navigation and positioning by carrying a sensor device, and can transmit the navigation information to the monitoring personnel through the wireless communication equipment; thus the safety of the emergency rescue personnel can be greatly guaranteed in an unknown environment. As an important branch of navigation, pedestrian navigation has attracted increasing attention from researchers.

At present, technologies suitable for pedestrian navigation can be divided into two technologies based on the Global Navigation Satellite System (GNSS) [1, 2] and on the radio frequency signal, positioning technology based on self-contained sensors. The first kind is relatively mature, but the signals are blocked by tall buildings, or when users are indoors, inside caves, or in jungles. The second kind based on the wireless frequency signal (such as WIFI RFID [3], UWB [4], etc.) requires pre-installing signal transmitting equipment in the positioning area, which is costly and has limited application range. It cannot be used in unknown environments and in the room where there is no signal transmitting device and signal receiving device. Personnel in dangerous occupations, such as firefighters and police officers, often operate in such environments and require precise localization in previously unknown surroundings. Compared with the other positioning

Citation
Wang, Y., & Wang B. (2024). Pedestrian Trajectory Reconstruction for Indoor Movement Based on Foot-Mounted IMU. *ICCK Transactions on Intelligent Systematics*, 1(1), 19–29.

© 2024 ICCK (Institute of Central Computation and Knowledge)

technologies based on self-contained sensors, the inertial measurement unit (IMU) has the advantage of strong independence, and mainly adopts sensors such as gyroscopes and magnetometers [5] or accelerometers and gyroscopes [6] to calculate pedestrian position information.

Thanks to the miniaturization technologies, such as MEMS (micro-electro-mechanical systems) or NEMS (nano-electro-mechanical systems), IMU becomes smaller, low-cost, and consume less power, and can be available to fix on the foot. Foot-mounted IMU has many indoor applications, including free-walking navigation for pedestrians in GPS-denied environments [7], such as anti-terrorism operations and fire rescue scenarios. For example, in the anti-terrorism application, the IMU system can provide the location to facilitate smooth conduct, which can improve the ability for the indoor cooperation of police groups and has great application value.

The main algorithm structure of the pedestrian navigation system is proposed by Foxlin E. [8] which is a shoe-mounted method using EKF (Extended Kalman Filter), ZUPT (Zero-Velocity Updates), and SINS (Strapdown Inertial Navigation System). Over the past few years, some researchers have tried to add another information source to this main algorithm structure such as building heading [9], prior maps [10], and visual odometer [11], to solve the problem of system error drift. However, the applications of these methods are limited only in some specific situations and the system accuracy is affected heavily by the selected sensors.

For the three-dimensional positioning of indoor floors, little research and accurate results are obtained. Due to the drift and integral error of IMU, the positioning results are very unstable, especially in the vertical direction. Because of the influence of gravity acceleration, there is a great deviation in the calculation of the height displacement. To solve this problem, some researchers use IMU to combine building structures, but firefighters execute rescue missions normally in emergencies and there are no prior maps. The visual sensor may be useless when it's dark or the environments are full of smoke. The conventional solution method is to use IMU with the barometer height to achieve vertical positioning of stairs [12], but the barometer is easily affected by temperature, airflow intensity and other factors in the fire and other harsh environments to realize the vertical height of the positioning accuracy.

This paper used an improved zero velocity detection algorithm to improve the accuracy of gait detection. Then, combined with the Kalman filter and zero velocity update algorithm to recognize gait accurately using our proposed linear gait discrimination method, on this basis, according to the results of gait discrimination, apply corresponding strategies. Finally, the accurate track between floors is obtained. The proposed method has been evaluated with walking experiments, and the comparable results have illustrated the effectiveness of the proposed algorithm of linear gait discrimination method. The error in the horizontal direction is less than 2%, and the error in the vertical direction is less than 2.5%. This method not only overcomes the redundancy associated with multi-sensor data fusion but also enables independent 3D trajectory reconstruction in complex unknown environments.

This paper is organized as follows. Section 2 introduced the system structure of the proposed PNS, including hardware structure and algorithm composition. Zero-velocity detection, which occupied an important role in the whole system was discussed in Section 3, and an improved zero-velocity detection algorithm was proposed. In Section 4, the attitude rotation matrix is described, then the prediction of pedestrian position and velocity, and the Kalman filter was used to update the attitude rotation matrix, position, and velocity. Based on the algorithm above, a linear gait discrimination method was proposed in Section 5, which can recognize gait effectively and obtain a 3D reconstructed trajectory. Section 6 shows the evaluation results of two sets of experiments. In Section 7, we give the main conclusions drawn from this work.

2 System structure

The PNS used in this paper only included one IMU, which is fixed in the left foot, as shown in Figure 1. The IMU adopted in our system is the MTi integrated sensor from Holland Xsens company (Figure 2). It contains a three-axis accelerometer, three-axis gyroscope, and three-axis magnetometer, which can be connected to the computer by RS232 interface or USB interface. The sampling rate is set at 100Hz, and its dynamic range is 600mg.

The PNS mainly consists of the following parts: an improved ZUPT algorithm is employed to more accurately determine when the foot is stationary. This



Figure 1. The IMU is fixed on the shoes.

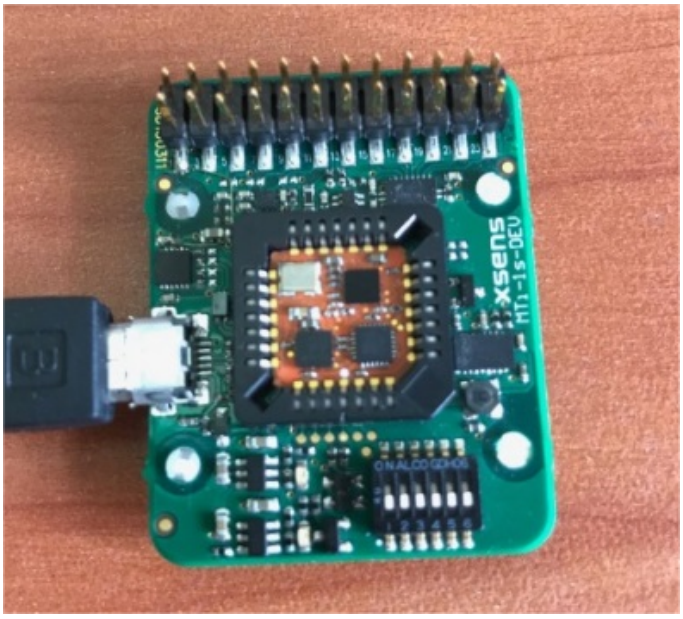

Figure 2. Xsens IMU.

could be used as a reference in the Kalman filter to correct the predicted position, velocity, and attitude angle of SINS. The linear gait discrimination method is used to judge the walking state of pedestrians and solve the inaccurate positioning problem on floor height estimation, realizing accurate indoor trajectory reconstruction. The algorithm architecture is shown in Figure 3.

3 Zero-velocity detection

3.1 Zero-velocity detection

Zero-velocity detection aims to determine whether the pedestrian's foot is in contact with the ground. The detected zero-velocity state could be used as the external measurement information for the system to reduce speed error and improve the positioning accuracy. Based on the signal source, the zero-velocity detection algorithm outputs one of two states: moving or static. Zero-velocity detection plays an important role in the whole system, as detailed in [13, 14].

In this study, a generalized likelihood ratio test (GLRT) algorithm is used, where the moving average variance of acceleration and the moving mean square value of angular velocity are used for zero-velocity determination.

The output of IMU was defined as

$$x_k = [x_k^a, x_k^w] \tag{1}$$

where $x_k^a, x_k^w \in \Omega^3$ are the specific acceleration and angular velocity measurement vectors respectively. By the Neyman-Pearson rule, we assume the value $Z_n = \{x_k, x_{n+1}, \ldots, x_{n+w-1}\}$, where n represents the sampling time and W represents the number of samples, we can get $T(Z_n)$ model as the following:

$$T(Z_n) = \frac{1}{W} \sum_{k=n}^{n+W-1} \left(\frac{1}{\delta_a^2} \left\| \bar{x}_k^a - g \frac{\bar{x}_k^a}{\|\bar{x}_k^a\|} \right\|^2 + \frac{1}{\delta_w^2} \|\bar{x}_k^w\|^2 \right) \tag{2}$$

where $T(Z_n)$ is the test statistics as shown in Figure 4 the red curves, g represents the gravity acceleration, $\bar{x}_k^a$ and $\bar{x}_k^w$ represent the mean of the samples respectively, δ_a^2 and δ_w^2 represent the noise variance of accelerometers and gyroscopes respectively.

In the stage of gait division, detection threshold $T_d(Z_n)$ needs to be pre-set, in this study, we set $T_d(Z_n) = 0.3 \times 10^5$, represented by the blue line in Figure 4, by comparing the detection statistic $T(Z_n)$ with the threshold $T_d(Z_n)$, the gait detection results are obtained. Gait detection results can be expressed as follows:

$$S_k = \begin{cases} 0, & \text{if } T(Z_n) > T_d(Z_n) \\ 1, & \text{if } T(Z_n) < T_d(Z_n) \end{cases} \tag{3}$$

where S_k stands for the detection result, corresponding to the black solid lines as shown in Figure 5. When $S_k = 1$ it indicates the static phase; while equal to 0, indicating the moving phase.

3.2 Improved zero-velocity detection algorithm

The pseudo-stance phase, induced by local fluctuations during the static phase, typically lasts only a short time and appears as noise in the detection result shown in Figure 5. The improved zero velocity detection algorithm adds a preset time threshold T_l based on the generalized likelihood ratio detection algorithm.

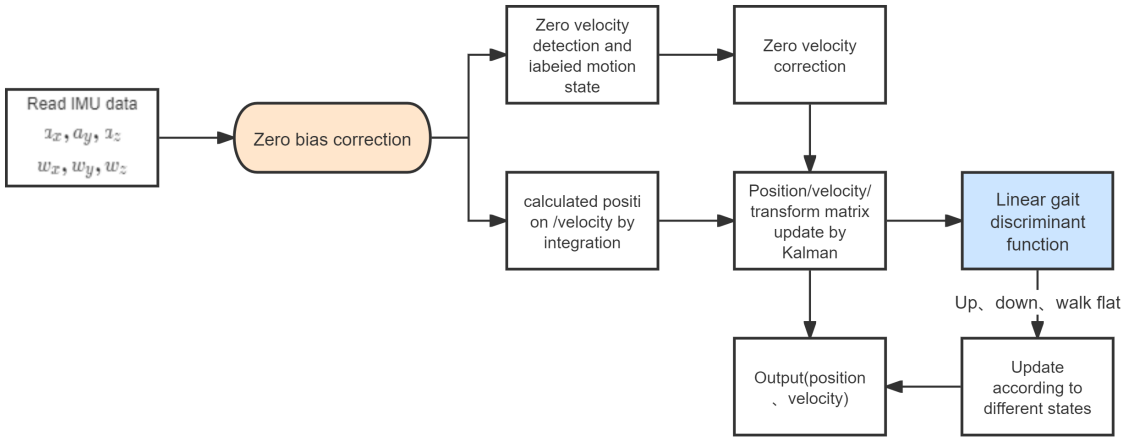

Figure 3. The algorithm architecture.

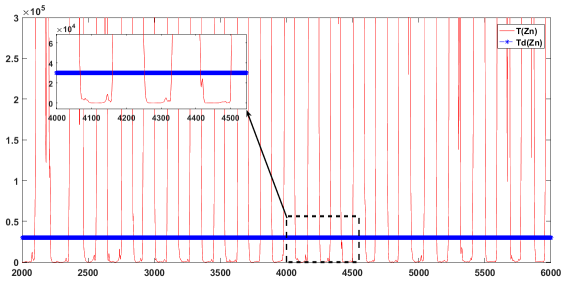

Figure 4. Judgement of zero velocity detection.

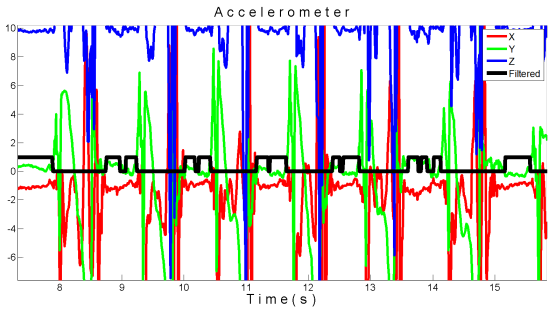

Figure 5. Gait recognition results based on zero velocity detection.

The improved zero velocity detection results can be expressed by the following formula:

$$S_k = \begin{cases} 0, & \text{if } L(T(Z_n) > T_d) > T_l \\ 1, & \text{if } L(T(Z_n) > T_d) < T_l \end{cases} \tag{4}$$

where $L(\cdot)$ represents the duration of gait phase. The modified gait detection result is shown in Figure 6. Traditional zero-velocity detection results contain a lot of pseudo-swing phases in the gait detection results, which results in inaccurate location calculation. The improved gait detection algorithm segments the gait effectively.

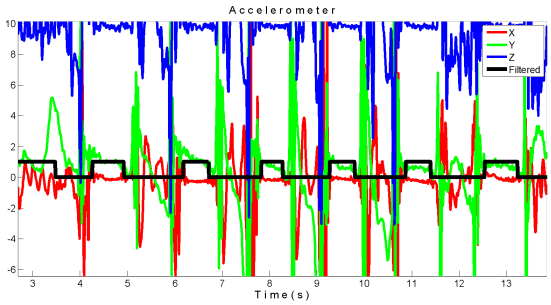

Figure 6. Gait recognition results based on improved ZUPT.

4 Position estimation based on Kalman Filter

After getting the result of gait detection, we need to estimate and correct the location of pedestrians through the zero-velocity reference combined with Kalman filter algorithm.

4.1 Calculation of attitude transform matrix

Data in body coordinate b and navigation coordinate n meets the following equation:

$$\begin{bmatrix} x_n & y_n & z_n \end{bmatrix} = C_b^n \begin{bmatrix} x_b & y_b & z_b \end{bmatrix} \tag{5}$$

where attitude transform matrix C_b^n represents the rotation relationship between the two coordinates, x_n, y_n, z_n represent the geographical coordinate of the east, north and up respectively, while x_b, y_b, z_b indicate the front, left and upward directions in body coordinate.

Therefore we can get the acceleration f of the navigation system as follows:

$$f = C_b^n \times \begin{bmatrix} \text{accX} & \text{accY} & \text{accZ} \end{bmatrix}^T - \begin{bmatrix} 0 & 0 & g \end{bmatrix}^T \tag{6}$$

where accX, accY, accZ represent the three-axis acceleration in body coordinate. Besides, f can be expressed as $[f(1) \quad f(2) \quad f(3)]^T$, which represent the acceleration along the $x_n, y_n \; and \; z_n$ axis respectively. Based on the acceleration of the navigation, we can get pedestrian location and speed information via integration computation. Therefore the accuracy of C_b^n, accX, accY and accZ will be very important to accurate pedestrian trajectory reconstruction.

The method of calculating the attitude matrix using quaternions has been extensively discussed in the literature [15]. Therefore, we only list the relevant equations as follows:

$$q = [q_0 \quad q_1 \quad q_2 \quad q_3]^T \tag{7}$$

Considering the relation between quaternions and gyro measurement data in body coordinate, the updated equation of quaternion is as follows. Suppose the quaternion is set as:

$$\dot{q}(t) = \frac{1}{2} M(w) q(t) \tag{8}$$

where $M(w)$ is given by

$$M(w) = \begin{bmatrix} 0 & -w_x & -w_y & -w_z \\ w_x & 0 & -w_z & w_y \\ w_y & w_z & 0 & -w_x \\ w_z & -w_y & w_x & 0 \end{bmatrix} \tag{9}$$

where w_x, w_y, w_z represent the X-axis, Y-axis, Z-axis angular velocity respectively.

According to equation (8), the quaternion matrix obtained through Pade-Baker method as the following:

$$q(t) = \left[\cos \frac{\Delta\theta_0}{2} I + \frac{\sin \frac{\Delta\theta_0}{2}}{\Delta\theta_0} \Delta\theta \right] q(0) \tag{10}$$

where $q(0)$ is the initial quaternion and $\Delta\theta$ denoted the change in angle, which can be got as follows:

$$\begin{aligned} \Delta\theta &= \int_t^{t+\Delta t} \Omega_{nb}^b(t)\, dt \\ &= \begin{bmatrix} 0 & -\Delta\theta_x & -\Delta\theta_y & -\Delta\theta_z \\ \Delta\theta_x & 0 & \Delta\theta_z & -\Delta\theta_y \\ \Delta\theta_y & -\Delta\theta_z & 0 & \Delta\theta_x \\ \Delta\theta_z & \Delta\theta_y & -\Delta\theta_x & 0 \end{bmatrix} \end{aligned} \tag{11}$$

$$\Delta\theta_0^2 = (\Delta\theta_x)^2 + (\Delta\theta_y)^2 + (\Delta\theta_z)^2 \tag{12}$$

where $\Delta\theta_x$, $\Delta\theta_y$, and $\Delta\theta_z$ are changes of angles, and can be obtained by $\Delta\theta_x = \omega_x \times \Delta t, \quad \Delta\theta_y = \omega_y \times \Delta t, \quad \Delta\theta_z = \omega_z \times \Delta t$. Then, the attitude transform matrix $C_{b_k}^n$ can be expressed in the form of a quaternion, as shown in equation (13).

$$C_{b_k}^n = \begin{bmatrix} 2(q_0^2 + q_1^2) - 1 & 2(q_1 q_2 - q_0 q_3) & 2(q_1 q_3 + q_0 q_2) \\ 2(q_1 q_2 + q_0 q_3) & 2(q_0^2 + q_2^2) - 1 & 2(q_2 q_3 + q_0 q_1) \\ 2(q_1 q_3 + q_0 q_2) & 2(q_2 q_3 - q_0 q_1) & 2(q_0^2 + q_3^2) - 1 \end{bmatrix} \tag{13}$$

4.2 Prediction of pedestrian position and velocity

Because the IMU exhibits inherent drift that accumulates over time, Kalman filter is applied here to correct the distortion. In a regular walking cycle, the IMU mounted on the foot will periodically swing. With the gait detection results, Kalman filter can better estimate the errors of attitude, velocity and position.

The model of zero velocity correction for Kalman filter is constructed as follows:

$$\dot{X} = FX + Gw \tag{14}$$

where X is the system state vector and defined as follows:

$$\dot{X} = [\delta_{s_x} \quad \delta_{s_y} \quad \delta_{s_z} \quad \delta_{v_x} \quad \delta_{v_y} \quad \delta_{v_z} \quad \delta_\rho \quad \delta_\xi \quad \delta_\psi]^T$$

where $\delta_{s_x}, \delta_{s_y}, \delta_{s_z}$ represent the error of position of target, $\delta_{v_x}, \delta_{v_y}, \delta_{v_z}$ is the error of velocity of target, and $\delta_\rho, \delta_\xi, \delta_\psi$ is the error of attitude angle. w is the process noise with the covariance Q_w.

In the state matrix, F is the matrix with 9 rows and 9 columns as the following

$$F = \begin{bmatrix} 0_{3\times3} & I_{3\times3} & 0_{3\times3} \\ 0_{3\times3} & 0_{3\times3} & f_m \\ 0_{3\times3} & 0_{3\times3} & 0_{3\times3} \end{bmatrix} \tag{15}$$

and f_m is structured as follows: (additional information on f_m structure would be specified here)

$$f_m = \begin{bmatrix} 0 & f(3) & -f(2) \\ -f(3) & 0 & f(1) \\ f(2) & -f(1) & 0 \end{bmatrix} \tag{16}$$

The discretized equation for (14) is as follows:

$$X_{k+1} = AX_k + w_k \tag{17}$$

where $A = I + F\Delta t + \frac{1}{2}(F\Delta t)^2$, X_k represents the state of moment k, w_k represents process noise. The covariance of w_k is calculated by Q_k.

$$\begin{aligned} Q_k = Qdt + \frac{1}{2}(FQ + QF^T)dt^2 \\ + \frac{1}{6}(2FQF^T + FFQ + QF^TF)dt^3 \end{aligned} \tag{18}$$

and Q is computed by $Q = G_k Q_w G_k^T$, G_w is from (14), G_k^T is a matrix with 9 rows and 6 columns and structured by $C_{b_k}^n$ from (13)

$$G_k = \begin{bmatrix} 0 & 0 \\ -C_{b_k}^n & 0 \\ 0 & C_{b_k}^n \end{bmatrix}$$

$$Z_k = HX_k + \tau_k \tag{19}$$

where Z_k is the measurement velocity; τ_k is the Gaussian white observation noise. H is the measurement matrix:

$$H = \begin{bmatrix} 0 & 0 & 0 & 1 & 0 & 0 & 0 & 0 & 0 \\ 0 & 0 & 0 & 0 & 1 & 0 & 0 & 0 & 0 \\ 0 & 0 & 0 & 0 & 0 & 1 & 0 & 0 & 0 \end{bmatrix} \tag{20}$$

Based on the output of the IMU, the errors in position, velocity, and attitude angle are estimated by the Kalman filter.

Firstly, the velocity and position are calculated with the acceleration f in the navigation coordinate obtained by equation (6) as follows:

$$\tilde{V}_k = V_{k-1} + f \times \Delta t \tag{21}$$

$$\tilde{S}_k = S_{k-1} + V_{k-1} \times \Delta t + \frac{1}{2} f \times \Delta t^2 \tag{22}$$

where $\tilde{V}_k$ is the velocity vector at time k, and $\tilde{V}_k = (v_x, v_y, v_z)$. $\tilde{S}_k$ is the position vector at time k, and $\tilde{S}_k = (s_x, s_y, s_z)$. V_{k-1} and S_{k-1} are estimated velocity and position at time $k-1$ respectively. Δt is the sampling time. It's known that $\tilde{V}_k$ and $\tilde{S}_k$ will gradually drift away from the true value due to the error of measured acceleration accX, accY, and accZ.

4.3 Update based on Kalman filter

After the Kalman filter predicted the velocity and position. There the zero-velocity information is used to correct the velocity, when we found the feet is in the stationary instant, we can use the measurement data:

$$Z_k = \begin{bmatrix} 0 & 0 & 0 \end{bmatrix}^T$$

Then by Kalman filter, we can get the updating process of the state as follows:

$$\hat{X}_{k,k} = \hat{X}_{k,k-1} + K_k(Z_k - H\hat{X}_{k,k-1}) \tag{23}$$

where $\hat{X}_{k,k-1}$ and $\hat{X}_{k,k}$ are the estimated state updated by the measurement Z_k. K_k is filter gain of Kalman filter, which can be calculated by the following

$$K_k = P_{k,k-1}H^T(R_k + HP_{k,k-1}H^T)^{-1} \tag{24}$$

the error covariance of the state estimation is calculated by the following

$$P_{k,k-1} = A_{k-1}P_{k-1,k-1}A_{k-1}^T + Q_{k-1} \tag{25}$$

The error covariance of the update process can be computed by

$$P_{k,k} = (I - K_k H)P_{k,k-1} \tag{26}$$

where $(k, k-1)$ refers to the predicted value from the sampling $k-1$ to k, (k, k) refers to the k point estimates, K_k is the filter gain, $P_{k,k-1}$ is the step prediction covariance.

We set the prediction error D, as $D = \hat{X}_{k,k} - \hat{X}_{k,k-1}$, D is a 9 dimensions vector and can be described as $D = [D(1)\ D(2)\ D(3)\ \ldots\ D(9)]$.

Then in the key part of the zero-velocity correction, according to the velocity calculated deviation correction position and speed.

$$S_k = \tilde{S}_k + \lambda D(1-3) \tag{27}$$

$$V_k = \tilde{V}_k + \lambda D(4-6) \tag{28}$$

where S_k is the position corrected at the k moment; V_k is the velocity corrected at the k moment. $D(1-3)$ are the 1st, 2nd, and 3rd elements of D, $D(4-6)$ are

the 4th, 5th, and 6th elements of D, and λ denotes the correction coefficient. By adjusting the value of λ, the errors of position and velocity can be adjusted. It needs to be pointed out that λ depends on the step length, which is related to the height of the pedestrian.

In order to correct the rotation matrix, the correction matrix is constructed as follows:

$$P_e = \begin{bmatrix} 0 & -D(9) & D(8) \\ D(9) & 0 & -D(7) \\ -D(8) & D(7) & 0 \end{bmatrix} \tag{29}$$

With the matrix above, the transform matrix $C_{b_k}^n$, can then be updated via the following equation:

$$C_{b_k}^n = (I + \beta P_e) \times C_{b_{k-1}}^n \tag{30}$$

where β is the coefficient according to the height of the moving pedestrian.

5 Linear gait discrimination method

In order to get the exact vertical height, this paper presents a method of linear discriminant function based on the pedestrian gait, each step is classified as stair climbing (ascending or descending) or flat walking using a linear discriminant function; it further determines whether the pedestrian is ascending or descending. Corresponding strategies are then applied based on the discriminant results. Specific methods are as follows:

The step size calculation formula is defined as follows:

$$d_{xy} = \sqrt{(x_{\text{end}} - x_{\text{start}})^2 + (y_{\text{end}} - y_{\text{start}})^2} \tag{31}$$

where d_{xy} is the displacement of each step, $(x_{\text{end}}, y_{\text{end}})$ is the surface coordinate of the last point during the moving phase, $(x_{\text{start}}, y_{\text{start}})$ is the surface coordinate of the initial position before the moving phase.

According to the actual measurement, when an adult walks on flat ground, the horizontal displacement per step is 0.9 m–1.15 m. When climbing stairs, if one step is taken at a time, the horizontal displacement is 0.3 m–0.38 m; if two steps are taken at a time, it is 0.6 m–0.75 m. It can be seen that the two scenes are very different in step size. We set the threshold $d_s = 0.8m$, by comparing horizontal displacements, to distinguish between taking the stairs and going flat.

If the direction of the vertical movement is necessary, some further rules need to be investigated as well. Here, the z axis displacement is calculated by using SINS. As we all know, the vertical displacement can't be obtained directly by integrating the z-axis acceleration, because there exists certain drifts, and it will significantly increase as time goes by. This is a known limitation of pure inertial navigation in the vertical direction. But through a large number of experiments, we found that although each time there will be drift, the computed values reliably reflect the ascending and descending trends. The indicator d_z could be computed as follows

$$d_z = z_{\text{end}} - z_{\text{start}} \tag{32}$$

where z_{start} and z_{end} are the coordinates in the vertical direction of the start and end points, the same as those in equation (31).

In summary, the linear gait discrimination function can be obtained:

$$l = \begin{cases} \text{upstairs}, & \text{if } d_{xy} < d_s, d_z > 0 \\ \text{downstairs}, & \text{if } d_{xy} < d_s, d_z < 0 \\ \text{walk flats}, & \text{if } d_{xy} > d_s \end{cases} \tag{33}$$

If the staircase is judged, the threshold is further set to judge whether to climb a step or two, setting another threshold as $d_{sl} = 0.5m$. If $d_z > d_{sl}$, then the z coordinate of the end point is assigned as z_{start} plus twice of the stair height that is $z_{\text{start}} + 2h$. If $d_z < d_{sl}$, then the z coordinate of the end point is assigned as z_{start} plus twice of the stair height that is $z_{\text{start}} + h$. If going downstairs, then $z_{\text{end}} = z_{\text{start}} - 2h$ or $z_{\text{end}} = z_{\text{start}} - h$, similarly to the upstairs. If the judgment result is to go flat, then set $z_{\text{end}} = z_{\text{start}}$, the h value needs to be calculated through multiple sets of data to test. At the beginning of the test, stair height calculation is accurate because the drift is weak, acceleration could be used for position computation in the vertical direction. Besides, with the relationship between z_{end} and z_{start}, the value h could then be determined. The height of a single stair, h, is calibrated from the first few steps. For example, if the first step is identified as a single step, then $h = z_{\text{end1}} - z_{\text{start1}}$. If it is identified as a double step, then the height of a single stair is calculated as $h = (z_{\text{end1}} - z_{\text{start1}})/2$. This calibrated value of h is then used in all subsequent height calculations.

The verification result of the proposed stair height calculation method was shown in Table 1. Three different bench heights were chosen as 0.15m, 0.16m,

and 0.165m, each group was verified by 20 sets of experiments, and the average stair height is used as the h value.

Table 1. Performance of the stair height calculation method.

Stair Height	0.15m	0.16m	0.165m
Calculated Average Stair Height h	0.1503m	0.1603m	0.1646m
Error	0.2%	0.19%	0.24%

6 Case study

In this section, two different cases were discussed to illustrate the effectiveness of the developed method. In case 1, positioning in the two-dimensional plane was considered, and reasonably accurate results were obtained. Furthermore, a three-dimensional scenario was implemented in case 2, where the performance of the linear gait discrimination method was verified.

Case 1

The experiment was conducted in the corridor No.3 Teaching Building in Beijing Technology and Business University (BTBU), as shown in Figure 7. After using the optimized zero velocity detection algorithm and selecting the appropriate parameters, the positioning results of the 2-dimensional horizontal plane are shown in Figure 8. The actual walking distance in the corridor was 39.6m, while the calculated value was 39.95m. In this case, the experimental error was 0.88%.



Figure 7. Experimental environment in case 1.

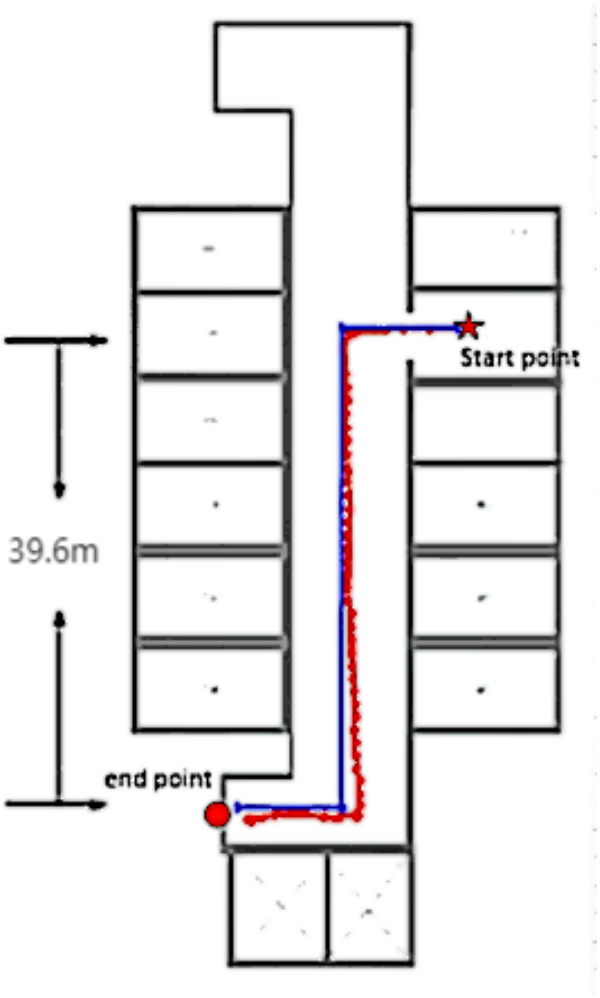

Figure 8. Two dimensional plane trajectory optimized by algorithm.

In case 2, the linear gait discrimination method was used to obtain accurate 3D indoor trajectory reconstruction. The experiment was carried out on the 6th floor of Gengyun Building in BTBU as shown in Figure 9.

Five persons of different heights, weights and genders were selected to carry out this experiment, and the height of the test personnel was between 160-185cm. During the test, the tester walked randomly through stairs and ground, and they were asked to their natural walking posture. The actual pedestrian walking posture and gait discrimination results are compared, and the comparison results are shown in Table 2. It could be seen that the error rate of the algorithm was less than 1.5%. The results show that the linear gait discrimination method proposed in this paper has a high recognition rate.

Case 2

The error rate is calculated by the formula

Table 2. Comparison results of actual pedestrian walking posture and discriminant results.

Participant	Up 1 step		Up 2 steps		Down 1 step		Down 2 steps		Flat ground	Error rate
	actual	test	actual	test	actual	test	actual	test		
Participant 1	15	14	78	80	21	20	52	55	210	1.86%
Participant 2	9	10	89	87	14	15	45	47	323	0.625%
Participant 3	15	14	58	61	19	18	103	105	403	0.84%
Participant 4	14	13	59	57	17	20	89	87	201	1.32%
Participant 5	8	9	78	81	17	15	105	101	326	1.12%

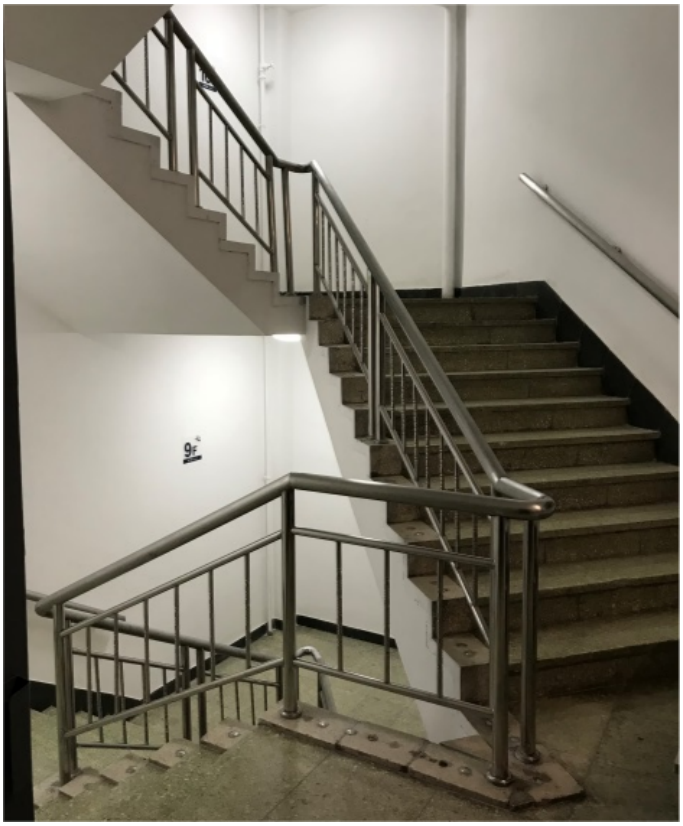

Figure 9. Experimental environment in case 2.

$$r_e = \frac{l_e}{L} \times 100\% \tag{34}$$

where r_e is the error rate, l_e represents the incorrect steps, and L is the number of actual walking steps, which is equal to the number of test steps.

The tester started from the sixth-floor staircase, ascended to the ninth floor, and then traversed a corridor distance. The actual floor height is 3.5 meters covering three stories, totaling 10.5 meters. We conducted three experiments:

Experiment 1: Employed only SINS without additional methods.

Experiment 2: Utilized a linear gait discrimination method.

Experiment 3: Integrated an Inertial Measurement Unit (IMU) and barometric pressure fusion to compute 3D pedestrian trajectory.

All experiments commenced from the coordinate origin (0,0,0).

The results of Experiment 1 are shown in Figure 10, we can see that the error is large, with a height drift of up to 13.5 m; Figure 11 shows the results of Experiment 2, the estimated floor height was 10.34 m; Figure 12 is the result of Experiment 3. The sampling interval of the barometer is 0.01 s, and the formula for calculating the height of the barometer is as follows

$$H = 44330 \times \left(1 - \left(\frac{p}{P_0}\right)^{0.19026}\right) \tag{35}$$

where H is the current height value of the calculation, p is the barometric value at the moment, and P_0 is the initial barometric value. This equation references the fusion method of Inertial Measurement Unit (IMU) and barometer[12]. Using this formula, the height calculation for the barometer results in 10.74 meters. The comparison of the three groups of experiments is shown in Table 3.

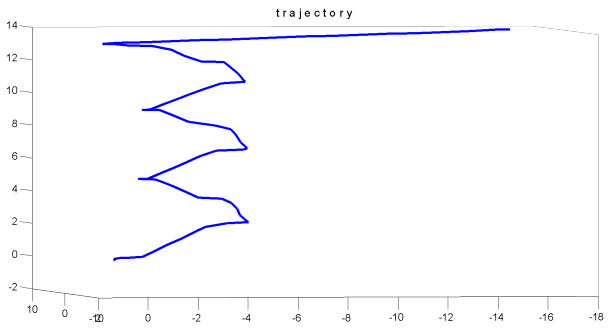

Figure 10. Only using SINS 3D indoor positioning results.

The above three experiments were carried out 30 times in each group, and the errors of Experiment 2 and Experiment 3 were within 2.5%. It can be seen that the proposed method achieves accuracy equivalent

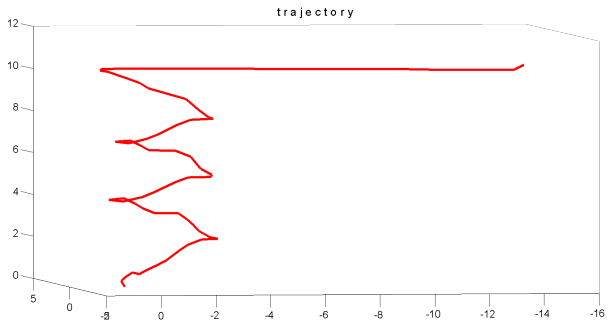

Figure 11. Three-dimensional positioning result map of pure ins using linear gait discriminant function.

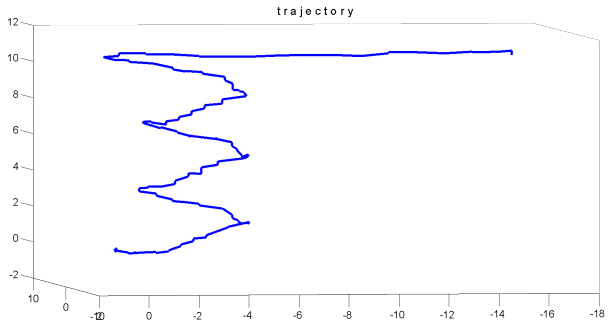

Figure 12. Results of data fusion using IMU and barometer.

to the IMU + barometer fusion approach, and even outperforms the latter in some cases. However, the barometer-based method has several drawbacks: it requires multiple sensors, which increases the complexity of data processing; the barometer reading fluctuates during flat walking due to instability; and in special environments such as fire scenes, the results are adversely affected by temperature changes and airflow. The proposed method uses only a single IMU, which not only eliminates the redundancy associated with multi-sensor fusion but also enables independent 3D trajectory reconstruction in complex unknown environments.

Table 3. The comparison of the three groups of experiments.

Experiment	Exp 1	Exp 2	Exp 3
Actual Height	10.5m	10.5m	10.5m
Test Height	13.5m	10.34m	10.74m
Error	28.6%	1.52%	2.28%

7 Conclusion

The foot-mounted IMU-based pedestrian indoor navigation is useful for various indoor applications such as finding and rescuing firefighters or other emergency first responders. This paper presented an improved zero velocity detection algorithm to obtain more accurate gait detection results. Then, the Kalman filter was combined with the zero velocity update algorithm to recognize gait accurately using our proposed linear gait discrimination method, on this basis, according to the results of gait discrimination, make corresponding strategies.

Finally, the accurate trajectory involving both horizontal and vertical movements between floors was obtained. Experimental results show that the proposed method achieves a horizontal error of less than 2% and a vertical error of 1.52% (with a maximum vertical error below 2.5% across all trials). This method not only overcomes the redundancy of multi-sensor fusion but also enables independent and robust 3D trajectory reconstruction using only a foot-mounted IMU. In future work, we will study more complicated movement cases, such as walking backwards, and sideways, as well as movement via the elevator.

Data Availability Statement

Data will be made available on request.

Funding

This work was supported without any funding.

Conflicts of Interest

The authors declare no conflicts of interest.

Ethical Approval and Consent to Participate

This study involved human participants recruited voluntarily for gait data collection in controlled experimental settings within the campus buildings of Beijing Technology and Business University (BTBU), China. All participants were fully informed of the experimental procedures, potential risks (including the physical demands of stair climbing across multiple floors), and their right to withdraw from the study at any time without consequence, prior to providing written informed consent. The experiments were conducted in compliance with the institutional research ethics guidelines of BTBU and in accordance with general ethical principles governing non-clinical human subjects research. Given the non-invasive and non-medical nature of the study — involving only the attachment of a foot-mounted IMU device and natural walking tasks — formal ethics committee review was not mandated under the applicable institutional policy. Nevertheless, all procedures were designed to minimize participant risk and discomfort. No

personally identifiable information was collected. Participant data were recorded solely in anonymized form, limited to gait motion measurements (step counts, trajectory coordinates, and height-related physical parameters), and were stored securely with access restricted to the research team. The study did not involve any medical interventions, health assessments, biological sampling, or collection of sensitive personal data. All participants provided voluntary informed consent and were free to withdraw at any stage.

References

[1] Basso, M., Galanti, M., Innocenti, G., & Miceli, D. (2020). Triggered INS/GNSS data fusion algorithms for enhanced pedestrian navigation system. *IEEE Sensors Journal, 20*(13), 7447-7459. [CrossRef]

[2] Lan, H., Yu, C., & El-Sheimy, N. (2015, April). An integrated PDR/GNSS pedestrian navigation system. In *China Satellite Navigation Conference (CSNC) 2015 Proceedings: Volume III* (pp. 677-690). Berlin, Heidelberg: Springer Berlin Heidelberg. [CrossRef]

[3] Xu, J., Li, Z., Zhang, K., Yang, J., Gao, N., Zhang, Z., & Meng, Z. (2023). The principle, methods and recent progress in RFID positioning techniques: A review. *IEEE Journal of Radio Frequency Identification*, 7, 50-63. [CrossRef]

[4] Sung, S., Kim, H., & Jung, J.-I. (2023). Accurate Indoor Positioning for UWB-Based Personal Devices Using Deep Learning. *IEEE Access*, 11, 20095-20113. [CrossRef]

[5] Ladetto, Q., & Merminod, B. (2002). Digital magnetic compass and gyroscope integration for pedestrian navigation. In *9th Saint Petersburg international conference on integrated navigation systems, Saint Petersburg, Russia*.

[6] Harle, R. (2013). A survey of indoor inertial positioning systems for pedestrians. *IEEE Communications Surveys & Tutorials, 15*(3), 1281-1293. [CrossRef]

[7] Wang, Q., Fu, M., Wang, J., Sun, L., Huang, R., Li, X., ... & Jiang, C. (2024). Free-walking: Pedestrian inertial navigation based on dual foot-mounted IMU. *Defence Technology, 33*, 573-587. [CrossRef]

[8] Foxlin E. (2005). Pedestrian Tracking with Shoe-Mounted Inertial Sensors. *IEEE Computer Graphics & Applications*, 25(6):38-46. [CrossRef]

[9] Cai, Y., Sun, Q., Zhang, Y., Yu, C., & Bai, H. (2016, October). Integrated navigation for pedestrian with building heading algorithm and inertial measurement unit. In *2016 International Conference on Control, Automation and Information Sciences (ICCAIS)* (pp. 167-170). IEEE. [CrossRef]

[10] Robertson, P., Angermann, M., Krach, B., & Khider, M. (2009, September). Inertial systems based joint mapping and positioning for pedestrian navigation. In *In Proceedings of the 22nd International Technical Meeting of the Satellite Division of The Institute of Navigation (ION GNSS 2009)*: 2096-2107).

[11] Jirawimut, R., Prakoonwit, S., Cecelja, F., & Balachandran, W. (2003). Visual odometer for pedestrian navigation. *IEEE Transactions on Instrumentation and measurement, 52*(4), 1166-1173. [CrossRef]

[12] Flores J Z, Farcy R. (2014). Indoor Navigation System for the Visually Impaired Using One Inertial Measurement Unit (IMU) and Barometer to Guide in the Subway Stations and Commercial Centers. In *International Conference on Computers for Handicapped Persons*. Springer, Cham:411-418. [CrossRef]

[13] Jimenez, A. R., Seco, F., Prieto, C., & Guevara, J. (2009, August). A comparison of pedestrian dead-reckoning algorithms using a low-cost MEMS IMU. In *2009 IEEE International Symposium on Intelligent Signal Processing* (pp. 37-42). IEEE. [CrossRef]

[14] Skog, I., Handel, P., Nilsson, J. O., & Rantakokko, J. (2010). Zero-velocity detection—An algorithm evaluation. *IEEE transactions on biomedical engineering, 57*(11), 2657-2666. [CrossRef]

[15] Shuster, M. D. (1993). A survey of attitude representations. *Journal of the Astronautical Sciences, 41*(4), 439-517. https://www.malcolmdshuster.com/Pub_1993h_J_Repsurv_scan.pdf



Yeqing Wang graduated from Beijing Technology and Business University in 2022 with a Bachelor's degree in Automation. He is currently a graduate student in Control Theory and Control Engineering at the same university. His research interests include pattern recognition and prediction, deep Learning, and related fields.



Binbin Wang graduated from Beijing University of Technology and Business in 2019 with a master's degree in Detection Technology and Automation Devices. His research focuses on pattern recognition and information fusion, unmanned vehicles, machine learning, and other related fields.